

A Novel Class of Ligand-gated Ion Channel Is Activated by Zn^{2+} *

Received for publication, August 28, 2002, and in revised form, October 9, 2002
Published, JBC Papers in Press, October 14, 2002, DOI 10.1074/jbc.M208814200

Paul A. Davies‡, Wei Wang§, Tim G. Hales‡¶, and Ewen F. Kirkness§||

From the ‡Department of Pharmacology and ¶Department of Anesthesiology and Critical Care Medicine, George Washington University Medical Center, Washington, D. C. 20037 and §The Institute for Genomic Research, Rockville, Maryland 20850

In mammals, the superfamily of “Cys loop,” ligand-gated ion channels (LGICs), is assembled from a pool of more than 40 homologous subunits. These subunits have been classified into four families representing channels that are gated by acetylcholine, serotonin, γ -aminobutyric acid, or glycine. By searching anonymous genomic sequence data for exons that encode characteristic motifs of the channel subunits, we have identified a novel LGIC that defines a fifth family member. Putative exons were used to isolate a full-length cDNA that encodes a protein of 411 amino acid residues. This protein (ZAC) contains all of the motifs that are characteristic of Cys loop channel subunits but cannot be assigned to any of the four established families on the basis of sequence similarity. Genes for ZAC are present in human and dog but appear to have been lost from mouse and rat genomes. Transcripts of ZAC subunits were detected in human placenta, trachea, spinal cord, stomach, and fetal brain. Transfection of human embryonic kidney cells with ZAC subunit cDNA caused expression of spontaneous current. By screening with a broad range of potential agonists and antagonists, we determined that tubocurarine inhibits the spontaneous current whereas Zn^{2+} activates the expressed receptors. The absence of Zn^{2+} -activated channels in rats and mice may explain why this fifth member of the LGIC superfamily has evaded detection until now.

Ion channels that are gated by acetylcholine, serotonin, γ -aminobutyrate, and glycine are a superfamily of homologous neurotransmitter receptors (nACh,¹ 5-HT₃, GABA_{A/C}, and glycine receptors, respectively). Each of these four receptor families is composed of multiple receptor subtypes derived from distinctive assemblies of five homologous subunits (1, 2). Although a wide variety of subunit genes has been identified in mammalian genomes (42 in human), each subunit can be assigned to one of the four receptor families on the basis of sequence similarity and, in most cases, functional activity. Many of these subunits confer unique properties to recombinant receptors in which they assemble, properties that have

often been poorly defined in prior studies of native tissues (3, 4). Consequently, the identification of novel receptor subunits continues to reveal unexpected properties of this receptor superfamily.

Most of the known subunits were identified by traditional methods of cross-hybridization or expression cloning. More recently, data bases of ESTs have been used to identify more distantly related homologues through computational searches for characteristic structural motifs (5–7). However, all of these methods have inherent limitations that can hinder the identification of a complete gene family. This is particularly relevant for subunits that are distantly related, that confer unexpected properties, and that are expressed at low levels in discrete locations or for short time periods during development. For such subunits, identification may only be possible through the analysis of a completely sequenced genome. Previously, during the early stages of sequencing the human genome, we used the draft sequence data to identify an elusive subunit of 5-HT₃ receptors (8). Here we have used a similar approach to uncover a very distinctive member of the subunit superfamily. This subunit cannot be assigned to any of the known receptor families on the basis of sequence similarity or functional properties. It appears to represent an old and distinct branch of the receptor superfamily that displays unique functional properties. Moreover, it also appears to be the first example of a subunit from this receptor superfamily that is expressed in human tissues but has been lost from at least some rodent species.

EXPERIMENTAL PROCEDURES

Isolation of the Human ZAC Subunit cDNA—A consensus peptide sequence of subunits for 5HT₃ and nACh receptors was used to search the nr and htgs data bases using the TBLASTN algorithm (www.ncbi.nlm.nih.gov/blast/). Homologous peptide fragments were identified within the six-frame translation of a human genomic DNA fragment (GenBank™ accession number AC018665). Oligonucleotide primers were designed from the genomic sequence to amplify the 5′- and 3′-flanking sequences from fetal brain and spinal cord cDNA libraries using the Marathon system (Clontech). Amplification at 95 °C for 45 s, 60 °C for 60 s, and 72 °C for 2 min was performed for 35 cycles using the XL-PCR system (PerkinElmer Life Sciences). Reaction products were purified from agarose gels and sequenced directly. The open reading frame of the new subunit cDNA (termed ZAC) was amplified from a spinal cord cDNA library as described above using primers containing nucleotides 1–21 (sense) and 1266–1289 (antisense) of the ZAC subunit cDNA sequence (GenBank™ accession number AF512521). The cloned product was sequenced over its entire length to ensure that no mutations had been introduced. Sequence alignments were generated by the ClustalW program from the MacVector package of sequence analysis software (Oxford Molecular Group). A cladogram was constructed using the neighbor-joining method with pairwise distances measured by absolute differences and gaps ignored. The bootstrap consensus was generated using 1,000 replications.

Northern Blot Analysis—Samples of ~2 μg of poly(A)⁺ mRNA (Clontech) underwent electrophoresis on a 1.2% formaldehyde agarose gel, were transferred to nylon membranes, and were hybridized with an

* The costs of publication of this article were defrayed in part by the payment of page charges. This article must therefore be hereby marked “advertisement” in accordance with 18 U.S.C. Section 1734 solely to indicate this fact.

The nucleotide sequence(s) reported in this paper has been submitted to the GenBank™/EBI Data Bank with accession number(s) AF512521–AF512523.

¶ To whom correspondence should be addressed: The Institute for Genomic Research, 9712 Medical Center Dr., Rockville, MD 20850. Tel.: 301-838-3536; Fax: 301-838-0208; E-mail: ekirknes@tigr.org.

¹ The abbreviations used are: nACh, nicotinic acetylcholine; GABA, γ -aminobutyric acid; 5-HT, 5-hydroxytryptamine; EST, expressed sequence tag; TC, tubocurarine; LGIC, ligand-gated ion channel; HEK, human embryonic kidney; GFP, green fluorescent protein.

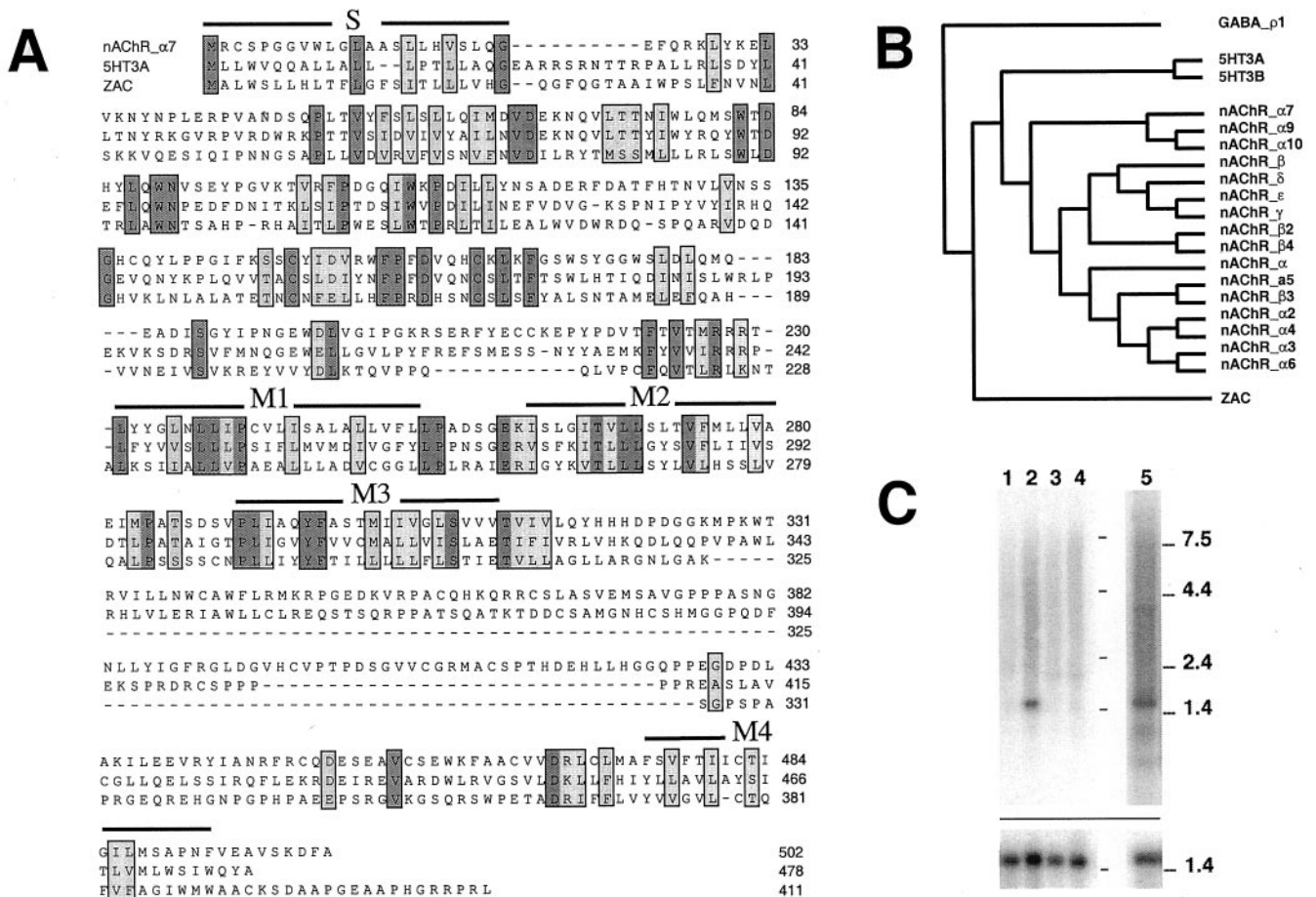


FIG. 1. Comparative sequence analysis and mRNA expression for the human ZAC subunit. *A*, alignment of human nAChR_α7, 5-HT_{3A}, and ZAC subunit sequences. Conserved residues are boxed and highlighted for identity (heavy shading) or chemical similarity (light shading). The potential signal sequence (S) and four putative transmembrane domains (M1–M4) are indicated by lines over the corresponding sequences. *B*, a cladogram of a ClustalW alignment of human subunit sequences that are homologous to residues 27–319 of the nACh receptor α subunit (nAChR_α). The distance matrix employed neighbor joining (12) with bootstrapping (1000 repetitions). The rooting outgroup was the GABA_A ρ1 subunit (GABA_ρ1). Branch points predict the order of divergence from a common ancestral gene. *C*, hybridization of poly(A)⁺ mRNA from small intestine (lane 1), placenta (lane 2), lung (lane 3), peripheral blood leukocytes (lane 4), and stomach (lane 5) with a ³²P-labeled riboprobe for the ZAC subunit (top panels). The same blots were probed with ³²P-labeled fragments of the human glyceraldehyde phosphate dehydrogenase cDNA (bottom panels).

antisense ³²P-labeled riboprobe that was derived from the ZAC subunit cDNA (nucleotides 1–447 of GenBank™ accession number AF512521). The blots were washed at 60 °C in 0.1× SSC, 0.1% SDS before exposure. The blots were stripped and reprobated with ³²P-labeled fragments of the glyceraldehyde-3-phosphate dehydrogenase cDNA (nucleotides 789–1140; Ref. 9).

Cloning of Orthologous Genomic Fragments from Mouse, Rat, and Dog—Fragments of genomic DNA were amplified using primer pairs that correspond to the 3′-ends of genes encoding the mouse, rat, and dog orthologues of the human galanin receptor 2 and KIAA1067 genes. For mouse and rat, these were 5′-CACCCGCACTTCCCACTGCACA and 5′-CTCATCATGGTGCCTGGTCAGGTA (nucleotides 1–23 and 5146–5169 of GenBank™ accession number AF512522). For dog, they were 5′-CCGACGGTTAATGCGACCTGAGGA and 5′-GGAGCAGGTGGGC-GACATGATCGA (nucleotides 1–24 and 5846–5869 of GenBank™ accession number AF512523). Aliquots of DNA (50 ng) from mouse, rat (Clontech), or dog (Novagen) were amplified using the XL-PCR system (Applied Biosystems). Reaction products were purified from agarose gels and sequenced directly.

Cell Culture and Transfection—HEK cells were grown in Dulbecco's modified Eagle's medium, supplemented with 10% calf serum, 100 IU/ml penicillin, and 100 μg/ml streptomycin. When cells approached confluence, they were seeded into 35-mm diameter dishes and transfected with cDNAs encoding the human ZAC subunit (in pcDNA1.1/amp) and GFP (in pCDM8). Cells were transfected using calcium phosphate precipitation (6). Cells were used 24–44 h after transfection.

Electrophysiology—The whole-cell patch-clamp technique was used

to record currents from HEK cells. The bath was continuously perfused (5 ml/min) with an extracellular solution containing (in mM): NaCl, 140; KCl, 4.7; MgCl₂, 1.2; CaCl₂, 2.5; glucose, 11; and HEPES, 10 (pH 7.4 with NaOH). The electrode solution contained (in mM): KCl, 140; MgCl₂, 2.0; EGTA, 11; and HEPES, 10 (pH 7.4 with KOH). The intracellular solution used to characterize the cation permeability of ZAC channels contained (in mM): KCl, 70; *N*-methyl-D-glucamine, 70; MgCl₂, 2.0; EGTA, 11; and HEPES, 10 (pH 7.4 with HCl). The intracellular solution used to determine the contribution of Cl[−] to the ZAC currents contained (in mM): KCl, 70; K⁺-gluconate, 70; MgCl₂, 2.0; EGTA, 11; and HEPES, 10 (pH 7.4 with KOH). Junction potentials were nulled prior to each experiment. Their inappropriate compensation was ignored in graphs of current-voltage relationships, but equilibrium potential values in the text were corrected. Cells were clamped at −60 mV unless otherwise stated. Drugs were applied either by pressure ejection from modified micropipettes or by bath perfusion. Experiments were performed at 22–24 °C.

Acquisition and Analysis of Data—Currents were amplified (Axopatch 200A, Axon Instruments), low pass-filtered at 1 kHz, and digitized (Digidata 1320, Axon Instruments, Foster City, CA) for acquisition onto the hard drive of a personal computer. Currents were averaged, superimposed, and measured using pCLAMP software (Axon Instruments). Zn²⁺ concentration-response data were obtained by prolonged (2 s) pressure ejection of randomized agonist concentrations from low resistance pipettes as described previously (10). Zn²⁺-activated currents often exhibited run-up. To compensate for this, 1 mM Zn²⁺ was applied before each concentration of Zn²⁺. The amplitudes of the Zn²⁺-activated currents were subsequently normalized to the cur-

FIG. 2. Spontaneous currents mediated by ZAC are blocked by TC. *A*, I_{spont} recorded from an HEK cell expressing recombinant ZAC appeared rapidly upon establishing the whole-cell configuration at -60 mV. Uncompensated capacitive currents appear during whole-cell recording in response to -5 mV steps. Leak currents were negligible in cells expressing GFP alone. *B*, TC ($100 \mu\text{M}$), applied with pressure for 2 s, reduced I_{spont} in cells expressing ZAC but had no effect on cells expressing GFP alone. *C*, the TC-inhibited current exhibits rectification. The TC-inhibited current amplitude was plotted against holding potential. Data points are average current amplitudes from three recordings normalized to the amplitude of currents recorded at -60 mV. Vertical bars represent \pm S.E.

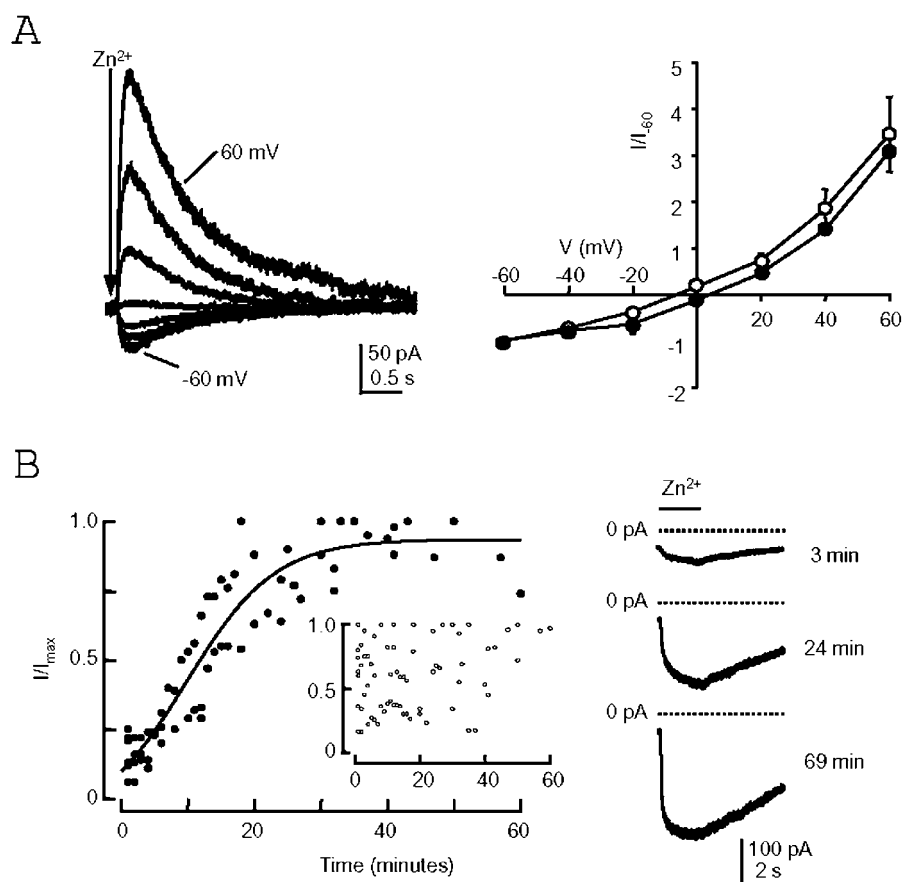
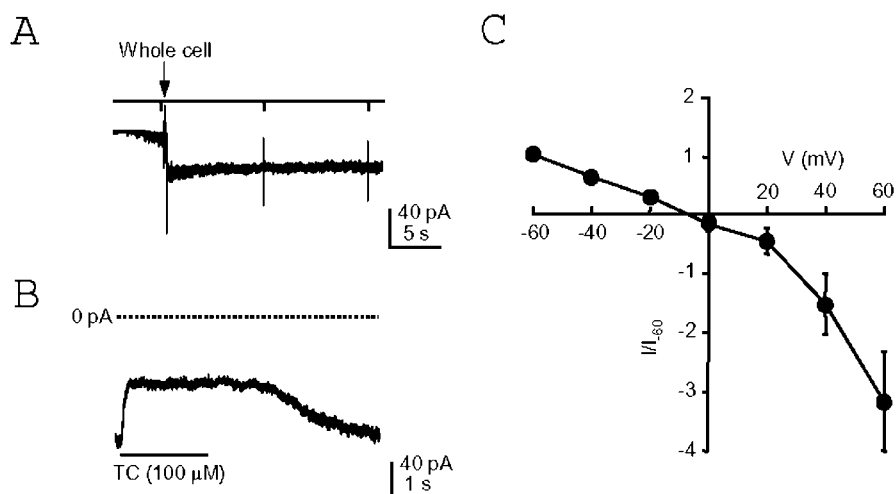


FIG. 3. Zn^{2+} activates ZAC. *A*, leak subtracted Zn^{2+} (1 mM)-activated currents, recorded from a cell expressing ZAC, with intracellular and extracellular solutions containing equal K^+ and Na^+ concentrations (~ 140 mM), respectively. Traces are averages of two currents recorded at each potential. The graph illustrates that I_{Zn} exhibited pronounced outward rectification with equilibrium potentials dependent on the concentration of intracellular K^+ . I_{Zn} were recorded from cells expressing ZAC with electrode solutions containing either 140 mM K^+ (open circles) or in which K^+ was substituted by equimolar NMDG $^+$ (70 mM; filled circles). *B*, a graph illustrating the time-dependent run-up of Zn^{2+} (1 mM for 2 s)-activated currents. Data points fitted with a sigmoidal function were I_{Zn} amplitudes at each time point normalized to the maximum I_{Zn} recorded from each cell ($n = 9$). The inset graph illustrates a lack of I_{spont} run-up recorded from the same cells. I_{spont} amplitudes were normalized to the maximum I_{spont} recorded from each cell. Representative current traces recorded from a single cell are shown in the right panel.

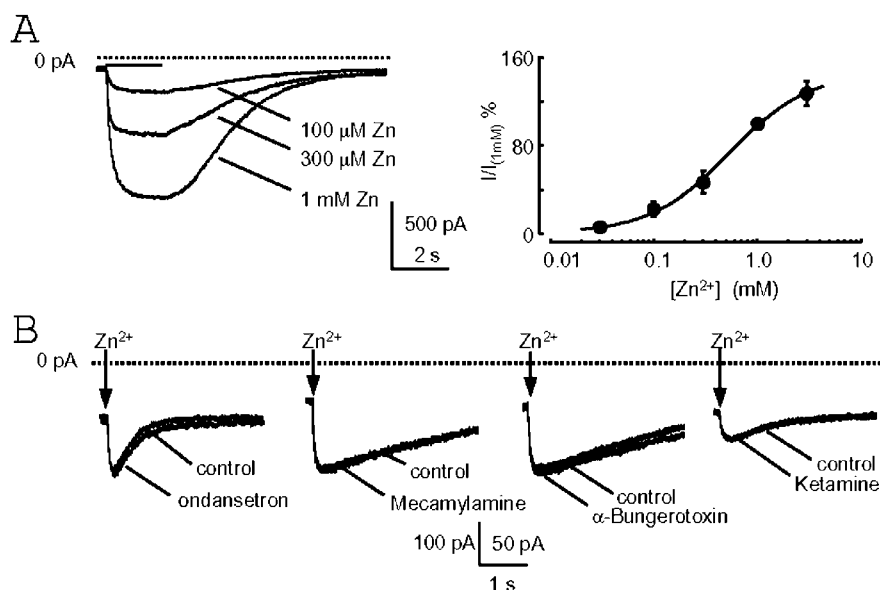
rent elicited by the prior application of 1 mM Zn^{2+} . Graphs of concentration-response relationships were fitted using the logistic function as described previously (10). Current-voltage relationships were analyzed by averaging at least two currents recorded at each holding potential. Individual current-voltage relationships were plotted, and a linear fit to points either side of current reversal yielded the equilibrium potential. All data are expressed as the arithmetic mean \pm S.E., and statistical comparisons were made using the Student's *t* test.

RESULTS

Cloning of the Human ZAC Subunit cDNA—Searches of the draft human genomic sequence with a consensus sequence of conserved residues revealed exons of a novel LGIC subunit within unannotated fragments of a bacterial artificial chromosome clone from chromosome 17q23. The exon sequences were

used to amplify flanking exons and a contiguous cDNA containing the complete open reading frame of the subunit. The subunit forms Zn^{2+} -activated channels (see below) and was termed ZAC. The ZAC subunit cDNA encodes a polypeptide of 411 amino acid residues (Fig. 1A). It has a signal sequence, a Cys-Cys motif, four predicted transmembrane domains, and several invariant residues that underpin the conserved secondary structure of the Cys loop LGIC superfamily (11). However, the sequence of the ZAC subunit is not closely related to any known subunits of this superfamily (maximum of 15% amino acid identity with 5-HT $_3\text{A}$ and nAChR $\alpha 7$ subunits; Fig. 1A). This is much lower than the level of identity between known subunits of 5-HT $_3$ receptors (30–40%) or nACh receptors (25–

FIG. 4. Concentration-dependent activation of ZAC by Zn^{2+} . A, exemplar Zn^{2+} -activated currents were recorded from the same cell and superimposed. Each trace is the average of three currents. A logistics fit to the Zn^{2+} concentration-response relationship yielded an EC_{50} of $540 \pm 9 \mu\text{M}$ ($n = 5$). Current amplitudes are expressed as percentage of those activated by 1 mM Zn^{2+} in each cell. Vertical bars represent \pm S.E. B, spontaneous and Zn^{2+} (1 mM)-evoked currents were unaffected by ondansetron (1 nM), mecamlamine ($10 \mu\text{M}$), α -bungarotoxin ($10 \mu\text{g/ml}$), and ketamine ($100 \mu\text{M}$). Each trace represents three currents averaged under control conditions or in the presence of the drugs indicated.



90%). Consequently, the ZAC subunit appears to represent a distinct species that diverged from the common ancestral subunit of the present day nACh and 5-HT₃ receptors (Fig. 1B).

A search of ZAC subunit cDNA and genomic sequences against human ESTs (www.ncbi.nlm.nih.gov/dbEST/index.html) revealed a surprisingly large number (>150) that contained exons of the ZAC subunit gene (encoding residues 181–411; Fig. 1A). However, almost all of these ESTs contain intronic sequences and are derived from mRNA that is transcribed in the opposite direction to the ZAC subunit mRNA. These ESTs represent transcripts of the KIAA1067 gene, which is located downstream of the ZAC subunit gene in the opposite orientation (see below, Fig. 6). The 3'-untranslated region of the KIAA1067 mRNA is complementary to both protein-coding and 3'-untranslated regions of the ZAC subunit mRNA and terminates within intron 5 of the ZAC subunit gene. Transcripts of the KIAA1067 gene are ubiquitous and abundant in human tissues. Reverse transcription/PCR, with primers from the first and last exons of the ZAC subunit gene, yielded a 1.27-kb ZAC subunit cDNA from prostate, thyroid, trachea, fetal whole brain, spinal cord, placenta, and stomach but not from adult whole brain, heart, liver, spleen, or kidney cDNA (data not shown). The presence of ZAC subunit mRNA (1.5 kb) in placenta and stomach was confirmed by Northern analysis, using an antisense riboprobe that was derived from the 5'-end of the ZAC subunit cDNA (Fig. 1C).

ZAC Subunits Form Homomeric Channels That Open Spontaneously—After transfection with ZAC and GFP cDNAs, HEK cells displayed spontaneous currents (mean amplitude = $-180 \pm 76 \text{ pA}$) immediately after achieving the whole-cell configuration at -60 mV . These were not seen in recordings from cells expressing GFP alone (Fig. 2A). This suggests that ZAC subunits form channels that can open in the absence of agonist. The existence of spontaneous current (I_{spont}) enabled us to screen for compounds that have either positive or negative intrinsic activity.

Agonists at other LGICs (GABA, glycine, glutamate, ATP, 5-HT, and acetylcholine; all at $100 \mu\text{M}$) lacked an ability to activate recombinant ZAC ($n \geq 5$). We also examined agonists of metabotropic receptors that are inactive at known mammalian LGICs (galanin, epinephrine, dopamine, histamine, neuropeptide Y, oxytocin, morphine, somatostatin, angiotensin II; all at $1 \mu\text{M}$). In addition, relatively nonspecific modulators of glutamate and GABA_A receptors were tested (glutathione (100

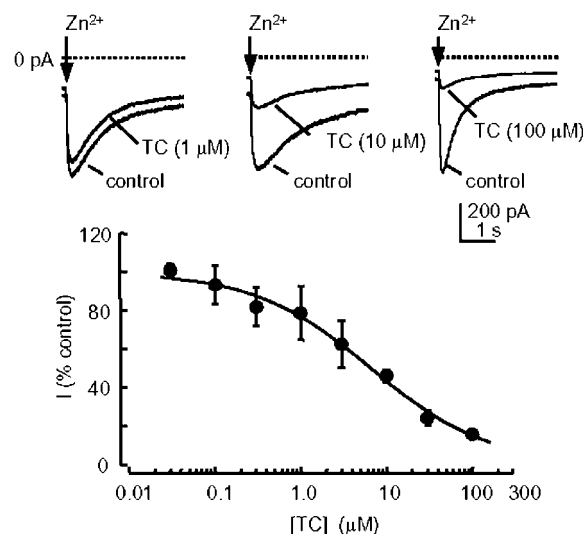


FIG. 5. TC inhibits ZAC activity. TC caused a concentration-dependent inhibition of I_{Zn} amplitude recorded from cells expressing ZAC. Exemplar Zn^{2+} (1 mM)-activated currents recorded from the same cell under control conditions and in the presence of TC are illustrated. Each trace is the average of three currents. A logistics fit to the TC (30 nM – $100 \mu\text{M}$) concentration-response relationship yielded an IC_{50} of $6.6 \pm 0.8 \mu\text{M}$ ($n = 4$). Current amplitudes are expressed as percentage of control. Vertical bars represent \pm S.E.

μM), ketamine ($100 \mu\text{M}$), allopregnanolone ($1 \mu\text{M}$), and propofol ($10 \mu\text{M}$)). None of these compounds affected membrane currents in cells expressing ZAC ($n \geq 3$).

In the absence of an agonist, we exploited the I_{spont} to test antagonists of related LGICs for negative activity at ZAC. When applied by bath, strychnine (100 nM), bicuculline methiodide ($10 \mu\text{M}$), α -bungarotoxin ($10 \mu\text{g/ml}$), mecamlamine ($10 \mu\text{M}$), and ondansetron (1 nM) had no effect on I_{spont} ($n \geq 2$). By contrast, TC ($100 \mu\text{M}$), a relatively nonselective inhibitor of nACh and 5-HT₃ receptors, inhibited I_{spont} when applied to the bath or by local pressure ejection ($n = 6$, Fig. 2B). The I_{spont} that was blocked by TC had an equilibrium potential of $-2 \pm 3 \text{ mV}$ ($n = 3$, Fig. 2C). Currents were larger at positive potentials than at corresponding negative potentials, indicating that I_{spont} is outwardly rectifying (Fig. 2C).

Zn^{2+} modulates several LGICs, often causing a potent inhi-

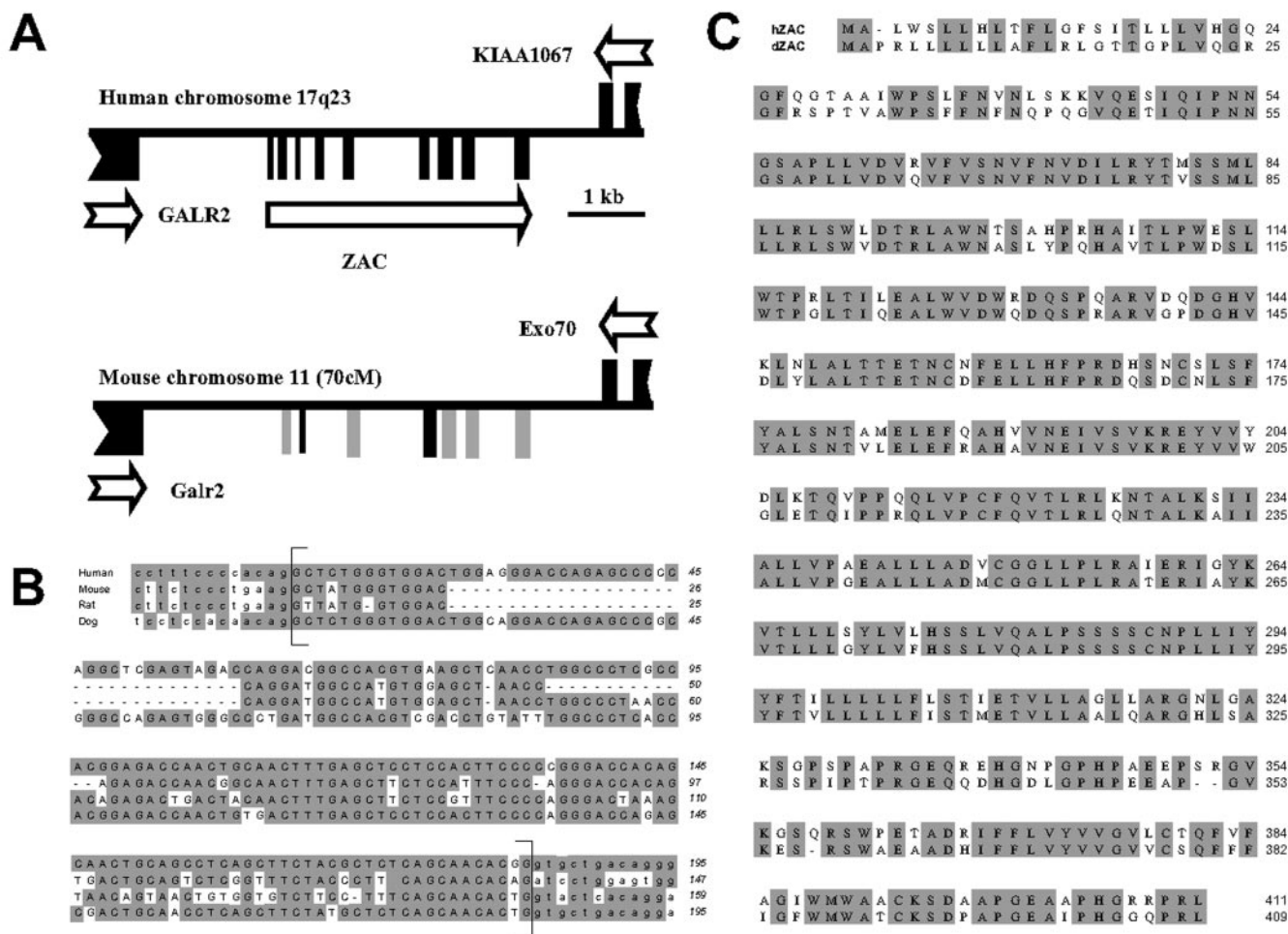


FIG. 6. A functional ZAC gene is absent from orthologous loci in rodents. *A*, the region of human chromosome 17q23 encoding the galanin2 receptor (GALR2), ZAC subunit, and the human orthologue of Exo70 (KIAA1067) was aligned with the orthologous region of mouse chromosome 11. Exons are indicated by black rectangles. Mouse exons that are homologous to human exons, but which contain insertions and deletions that generate in-frame stop codons, are indicated in gray. *B*, the sequence of exon 5 from the human ZAC subunit gene is aligned with orthologous sequences from mouse, rat, and dog genomic DNA. For the human sequence, exon 5 is in uppercase, inside brackets. Nucleotides that are conserved between human and other species are shaded. *C*, alignment of the deduced amino acid sequences for the human and dog ZAC subunits (hZAC subunit and dZAC subunit, respectively). Conserved residues are shaded.

bition of channel activity (13). Surprisingly, the local application of Zn^{2+} (1 mM) caused activation of inward currents in cells expressing ZAC (Figs. 3–5) but not in cells expressing GFP alone ($n = 4$).

Activation of ZAC Channels by Zn^{2+} — Zn^{2+} -activated currents (I_{Zn}) had an equilibrium potential (E_{Zn}) of -5 ± 1 mV ($n = 6$) and outward rectification similar to that of I_{spont} (Figs. 2C and 3A). We used alternative electrode solutions to examine the ionic selectivity of ZAC. Substitution of half the intracellular K^+ with *N*-methyl-D-glucamine (70 mM), caused a right shift in the current-voltage relationship (Fig. 3A), producing a positive Zn^{2+} equilibrium potential (2 ± 3 mV, $n = 3$). This demonstrates a role for intracellular K^+ ions in I_{Zn} . Substitution of half of the intracellular K^+Cl^- with K^+ -gluconate (70 mM) had no significant effect on Zn^{2+} equilibrium potential ($n = 4$), demonstrating that the channels have negligible Cl^- permeability.

There was little correlation between the amplitudes of I_{Zn} and I_{spont} in cells expressing ZAC. Furthermore, run-up of I_{Zn} was frequently observed during an experiment without a corresponding change in the amplitude of I_{spont} (Fig. 3B). These observations suggest that Zn^{2+} activates channels that are closed prior to its application. In cells expressing ZAC, Zn^{2+} caused a concentration-dependent activation of currents, with

a threshold of $\sim 30 \mu\text{M}$ and an EC_{50} of $540 \pm 9 \mu\text{M}$ (Fig. 4A). As with the I_{spont} , I_{Zn} was insensitive to bath-applied α -bungarotoxin (10 $\mu\text{g}/\text{ml}$), mecamylamine (10 μM), ondansetron (1 nM), and ketamine (100 μM ; Fig. 4B). By contrast, TC caused a concentration-dependent inhibition of I_{Zn} (Fig. 5) with an IC_{50} of $6.6 \pm 0.8 \mu\text{M}$ ($n = 4$).

Absence of Functional ZAC Subunit Genes in Rodents—We were unable to amplify fragments of an orthologous gene from mouse or rat genomic DNA using degenerate primers designed from the ZAC amino acid sequence (data not shown). More surprisingly, searches of the draft mouse and rat genomic sequences (www.celera.com and www.ncbi.nlm.nih.gov) failed to yield fragments of orthologous genes. The human ZAC gene is located between genes encoding the galanin2 receptor and KIAA1067 (Fig. 6A). Consequently, we amplified and sequenced the region between the orthologues of these two genes from mouse, rat, and dog genomic DNA. For all four species, there is detectable homology between the DNA sequences of this region. This is most apparent where the human sequence represents an exon of the ZAC gene (Fig. 6B). However, for mouse and rat, most of the fragments that are homologous to exons of the human ZAC subunit gene contain numerous insertions, deletions, and substitutions that introduce in-frame stop codons (Fig. 6B). Only a footprint of the ZAC gene remains

in these species, and they are no longer capable of expressing a functional ZAC subunit. In contrast, dog genomic DNA from this region encodes a full-length ZAC subunit that displays 84% amino acid conservation with the human ZAC subunit (Fig. 6C).

DISCUSSION

The ZAC subunit displays all of the structural motifs that are common to the superfamily of Cys loop LGICs. However, its distinctive sequence and function prevent its classification within any of the four established receptor families. Sequence analysis indicates that a common ancestral gene gave rise to the present day ZAC, nACh, and 5-HT₃ receptor subunit genes. Since they diverged, a functional ZAC subunit gene has been retained by some mammals (e.g. human and dog) but has been lost by others (e.g. mouse and rat). Most human genes, including those for all previously identified LGIC subunits, have rodent orthologues. However, there is evidence for a differential loss of a limited number of genes from either rodent or human genomes (e.g. Refs. 14 and 15). With respect to ZAC, this raises the possibility that humans and rodents differ in some fundamental cell signaling mechanisms. To date, the properties of endogenous LGICs have been studied predominantly in rodent cells. An absence of ZAC from mice and rats may explain why its unusual properties have not been described previously.

ZAC exhibits TC-sensitive spontaneous activity. Some nACh and GABA_A receptor subtypes are also spontaneously active, either in their natural environment (16) or when expressed in recombinant systems (17). Persistent GABA_A channel openings attenuate cellular excitability and can contribute to the maintenance of resting membrane potential (18). Spontaneous nACh channel activity may participate in embryonic muscle development (16). The physiological role of spontaneous ZAC remains to be determined. However, the ability of TC to block this activity will be useful for characterizing the properties of native ZAC in tissue preparations.

Zn^{2+} causes a concentration-dependent activation of ZAC. Zn^{2+} can also modulate the activity of related LGICs, although, in most cases, it inhibits channel function (19–22). However, at the glycine receptor, its effect is biphasic, potentiating glycine-evoked responses at low concentrations and inhibiting them at higher concentrations (20). Zn^{2+} may activate ZAC through an action at the putative N-terminal loop B ligand-binding domain. Subunits of each LGIC family display characteristic loop B residues that may reflect a role in agonist selectivity (11). Notably, the relevant loop B residues in the ZAC subunit (Leu-177 and Asn-179) are distinct from the corresponding residues of related subunits. This also suggests that ZAC represents a distinct class of Cys loop LGICs. It is also possible that Zn^{2+} activates ZAC through an allosteric site that is unrelated to the loop B motif. This would be analogous to the direct activation of GABA_A receptors by general anesthetics (23).

A relatively high concentration of Zn^{2+} ($>30 \mu\text{M}$) is required for activation of ZAC. Zn^{2+} is concentrated in various tissues, including the forebrain, testes, and neuroendocrine cells (24, 25). In the hippocampus, pituitary, and pancreatic β -cells, Zn^{2+}

is concentrated in vesicles at high concentrations ($>1 \text{ mM}$; Ref. 25). During vesicular release, it is possible that micromolar concentrations of Zn^{2+} are present within the synaptic cleft. However, high affinity binding to extracellular albumin is likely to reduce free Zn^{2+} concentrations to the low nanomolar range within a short distance from its source. Native ZAC may be located close to a vesicular source of free Zn^{2+} . Indeed, fetal brain is among a variety of human tissues that express transcripts of the ZAC subunit. Expression of ZAC subunit mRNA was detectable in several other human tissues. However, the absence of a functional ZAC subunit gene in rats and mice precludes the use of these rodents for more detailed localization studies. To resolve the distribution of ZAC expression at the cellular level, it will be necessary to perform such studies on tissues from human, dog, or other non-rodent species.

It is possible that, in its native environment, the affinity of ZAC for Zn^{2+} is increased by a cofactor or by post-translational modification. The observed run-up of I_{Zn} indicates an increased ability of Zn^{2+} to activate the channel during the course of an experiment. Future experiments will examine whether this phenomenon is caused by post-translational regulation. It is also possible that Zn^{2+} is not the physiological agonist for ZAC. However, with the knowledge that Zn^{2+} behaves as an agonist and TC as an inhibitor of spontaneous gating, these agents will be useful tools for characterizing the properties of native ZAC receptors in tissues from human and other non-rodent species.

REFERENCES

1. Karlin, A. (2002) *Nat. Rev. Neurosci.* **3**, 102–114
2. Reeves, D. C., and Lummis, S. C. (2002) *Mol. Membr. Biol.* **19**, 11–26
3. Paterson, D., and Nordberg, A. (2000) *Prog. Neurobiol.* **61**, 75–111
4. Mohler, H., Crestani, F., and Rudolph, U. (2001) *Curr. Opin. Pharmacol.* **1**, 22–25
5. Hedblom, E., and Kirkness, E. F. (1997) *J. Biol. Chem.* **272**, 15346–15350
6. Davies, P. A., Hanna, M. C., Hales, T. G., and Kirkness, E. F. (1997) *Nature* **385**, 820–823
7. Lustig, L. R., Peng, H., Hiel, H., Yamamoto, T., and Fuchs, P. A. (2001) *Genomics* **73**, 272–283
8. Davies, P. A., Pistis, M., Hanna, M. C., Peters, J. A., Lambert, J. J., Hales, T. G., and Kirkness, E. F. (1999) *Nature* **397**, 359–363
9. Tokunaga, K., Nakamura, Y., Sakata, K., Fujimori, K., Ohkubo, M., Sawada, K., and Sakiyama, S. (1987) *Cancer Res.* **47**, 5616–5619
10. Adodra, S., and Hales, T. G. (1995) *Br. J. Pharmacol.* **115**, 953–960
11. Brejc, K., van Dijk, W. J., Klaassen, R. V., Schuurmans, M., van Der Oost, J., Smit, A. B., and Sixma, T. K. (2001) *Nature* **411**, 269–276
12. Saitou, N., and Nei, M. (1987) *Mol. Biol. Evol.* **4**, 406–425
13. Harrison, N. L., and Gibbons, S. J. (1994) *Neuropharmacology* **33**, 935–952
14. Mural, R. J., Adams, M. D., Myers, E. W., Smith, H. O., Miklos, G. L., Wides, R., Halpern, A., Li, P. W., Sutton, G. G., Nadeau, J., et al. (2002) *Science* **296**, 1661–1671
15. Morinaga, T., Nakakoshi, M., Hirao, A., Imai, M., and Ishibashi, K. (2002) *Biochem. Biophys. Res. Commun.* **294**, 630–634
16. Jackson, M. B. (1984) *Proc. Natl. Acad. Sci. U. S. A.* **81**, 3901–3904
17. Davies, P. A., Kirkness, E. F., and Hales, T. G. (2001) *J. Physiol. (Lond.)* **537**, 101–113
18. Brickley, S. G., Revilla, V., Cull-Candy, S. G., Wisden, W., and Farrant, M. (2001) *Nature* **409**, 88–92
19. Smart, T. G., and Constanti, A. (1990) *Br. J. Pharmacol.* **99**, 643–654
20. Bloomenthal, A. B., Goldwater, E., Pritchett, D. B., and Harrison, N. L. (1994) *Mol. Pharmacol.* **46**, 1156–1159
21. Gill, C. H., Peters, J. A., and Lambert, J. J. (1995) *Br. J. Pharmacol.* **114**, 1211–1221
22. Palma, E., Maggi, L., Miledi, R., and Eusebi, F. (1998) *Proc. Natl. Acad. Sci. U. S. A.* **95**, 10246–10250
23. Amin, J., and Weiss, D. S. (1993) *Nature* **366**, 565–569
24. Vallee, B. L., and Falchuk, K. H. (1993) *Physiol. Rev.* **73**, 79–118
25. Frederickson, C. J., Suh, S. W., Silva, D., Frederickson, C. J., and Thompson, R. B. (2000) *J. Nutr.* **130**, (suppl.) 1471–1483